Imagery and initial results from the Terra Multi-angle Imaging SpectroRadiometer (MISR)

David J. Diner and the MISR Science Team
Jet Propulsion Laboratory, California Institute of Technology, Pasadena, CA 91109

ABSTRACT

The Multi-angle Imaging SpectroRadiometer (MISR) instrument was launched into polar orbit aboard the Terra spacecraft in December 1999, and collection of Earth imagery began in February 2000. MISR contains nine cameras pointed at fixed along-track directions, and acquires images with view angles at the Earth's surface ranging from 70.5° forward of nadir to 70.5° aftward. Each camera contains four CCD line arrays filtered to blue, green, red, and near-infrared wavelengths. Spatial sampling ranging from 275 m to 1.1 km is obtained over a 400-km swath width. Each area observed by MISR is imaged at all nine angles within a seven-minute period. MISR provides a unique approach to characterizing atmospheric aerosols, the surface, and clouds. This paper provides examples of MISR products derived from imagery acquired during the first six months of data collection.

Keywords: Terra, MISR, multi-angle, imaging, remote sensing

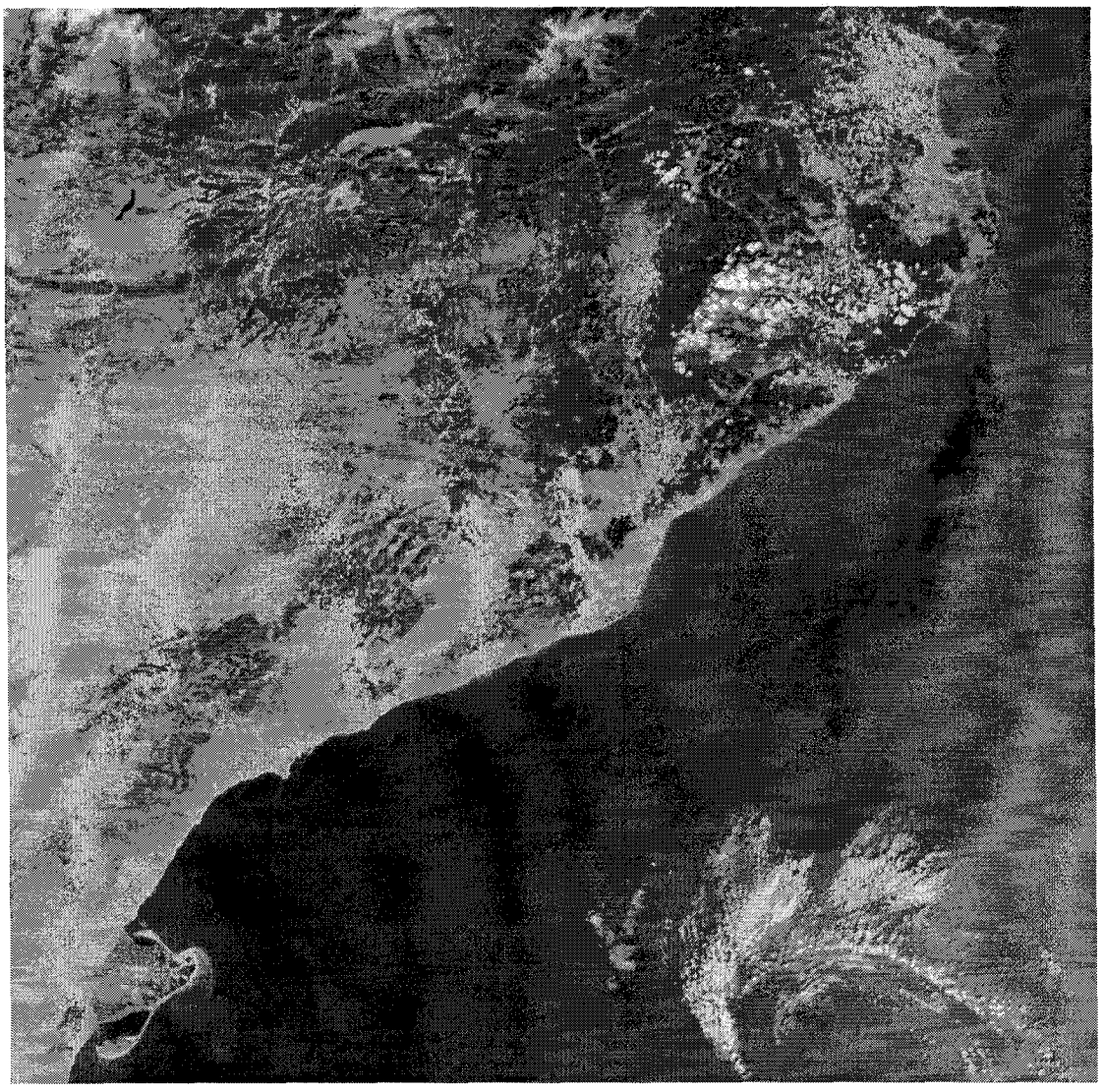

Figure 1. MISR nadir camera image of northeastern Spain including the city of Barcelona, the location of the Europto Symposium on Remote Sensing. The image was acquired on June 7, 2000. North is at the top.

1. INTRODUCTION

The MISR instrument[1] was launched into polar Earth orbit aboard the Terra spacecraft on December 18, 1999. Terra is in a 16-day repeat 705-km sun-synchronous orbit, and has approximately a 10:45 am equator crossing time on the descending node. MISR provides multiple-angle, continuous imagery of the Earth in reflected sunlight. It uses nine separate charge coupled device (CCD)-based pushbroom cameras to observe the Earth at nine discrete angles: one at nadir, plus eight other symmetrically placed cameras that provide fore-aft observations with view angles, at the Earth's surface, of 26.1°, 45.6°, 60.0°, and 70.5° relative to the local vertical. Imagery in four spectral bands (blue, green, red, and near-infrared) is provided at each angle, yielding a total of 36 image channels (9 angles x 4 bands). MISR measurements are designed to improve our understanding of the Earth's ecology, environment, and climate. A detailed understanding of how sunlight is scattered in different directions is necessary in order to determine how changes in the amounts, types, and distribution of clouds, airborne particulates, and surface cover affect our climate.

Table 1 summarizes top-level instrument specifications. The spatial resolution of the instrument is commandable, through flight software, to 275 m, 550 m, or 1.1 km. The nominal global observing mode of the instrument provides 275-m resolution in all bands of the nadir camera and the red band of each of the off-nadir cameras, and 1.1 km for the remaining 24 channels.

Table 1. MISR instrument system as-built specifications

Parameter	As-Built
Spectral Bands (solar weighted in-band response)	446.4 nm (Blue) 557.5 nm (Green) 671.7 nm (Red) 866.4 nm (Near-Infrared)
Spectral Bandwidths (solar weighted in-band response)	41.9 nm (Blue) 28.6 nm (Green) 21.9 nm (Red) 39.7 nm (Near-Infrared)
Data Rate (orbital average)	3.3 Mbps
Quantization	14 bits linear, square-root compressed to 12 bits
Swath width	~400 km, providing 9-day global coverage
Spatial resolution (commandable)	275 m - 1.1 km

MISR's cameras have progressively increasing focal lengths as the view angle increases in order to preserve cross-track resolution as a function of angle. A nomenclature has been devised to provide a shorthand way of referring to the individual cameras. The designation An is used for the nadir view; the forward-viewing four cameras are designated Af, Bf, Cf, and Df in order of increasing off-nadir angle; and the aftward-viewing bank is designated Aa, Ba, Ca, and Da. Here, A, B, C, D refer to the effective focal lengths of the camera lenses (approximately 59, 73, 95, and 124 mm, respectively). The A design is used for the nadir as well as near-nadir cameras, providing slightly higher resolution in the raw nadir camera imagery; however, the resampled and georectified data are placed on equal scale grids. On-board calibration hardware provides high radiometric accuracy and stability of the data. This observing strategy enables the rigorous use of radiative transfer theory and physically-based models to facilitate the retrieval of cloud, aerosol, and surface properties. Figure 2 is a rendering of the MISR instrument measurement approach.

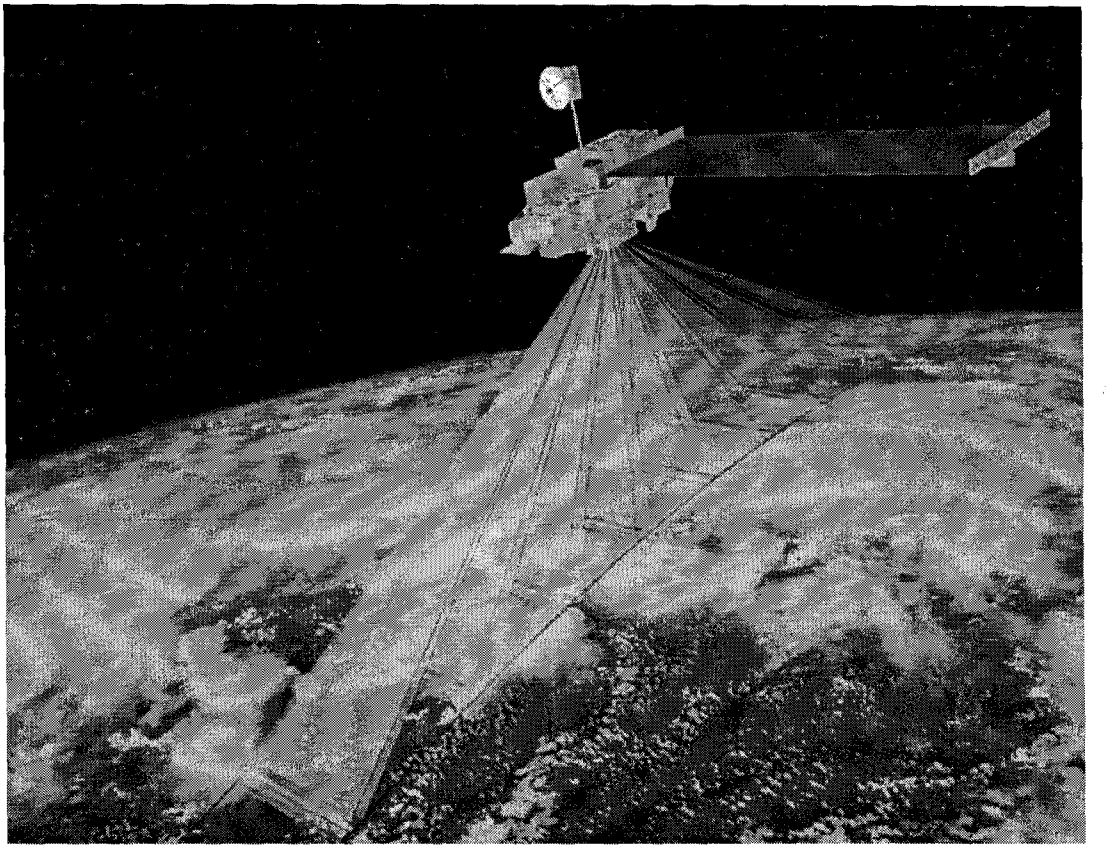

Figure 2. Rendering of the MISR along-track pushbroom imaging approach.

The MISR Science Computing Facility (SCF) at JPL and the Atmospheric Sciences Data Center (ASDC) Distributed Active Archive Center (DAAC) at NASA Langley Research Center represent the primary entities in which the functions of MISR science data processing are implemented. The LaRC DAAC, which is shared with several other Earth Observing System (EOS) instruments, is the facility at which software incorporating MISR science algorithms operates in a high volume, real-time mode to produce standard science data products.

Standard product generation at the DAAC is dependent on calibration parameters and other look-up data, such as threshold datasets, atmospheric climatologies, aerosol and surface model datasets and the like. These are produced at the SCF. Updates to these data structures occur infrequently compared to the rate of standard product generation, and therefore fit into the more limited processing capabilities of the SCF. Other essential functions that have activities at the SCF include quality assessment, algorithm and data product validation, software development, and instrument operations.

2. IN-FLIGHT IMAGERY

The Terra spacecraft reached final orbit on February 23, 2000 and the MISR instrument cover was opened the next day. "First light" imagery was acquired while the Df camera was viewing James Bay at the southern end of Hudson Bay in the Ontario-Quebec region of Canada. A set of multi-angle imagery of this area is shown in Figure 3. The abrupt transition from dark to light in the Df image marks the opening of MISR's cover as this camera was viewing the scene. The image acquired by the nadir camera was obtained about 3.5 minutes later, and the aftward image was acquired about 7 minutes after the forward view. Changes in brightness and contrast with angle distinguish different environmental conditions, notably the fast (smooth) ice whose glint-like reflection makes it brighter in the forward view, pack (rough) ice which is more backscattering, and clouds.

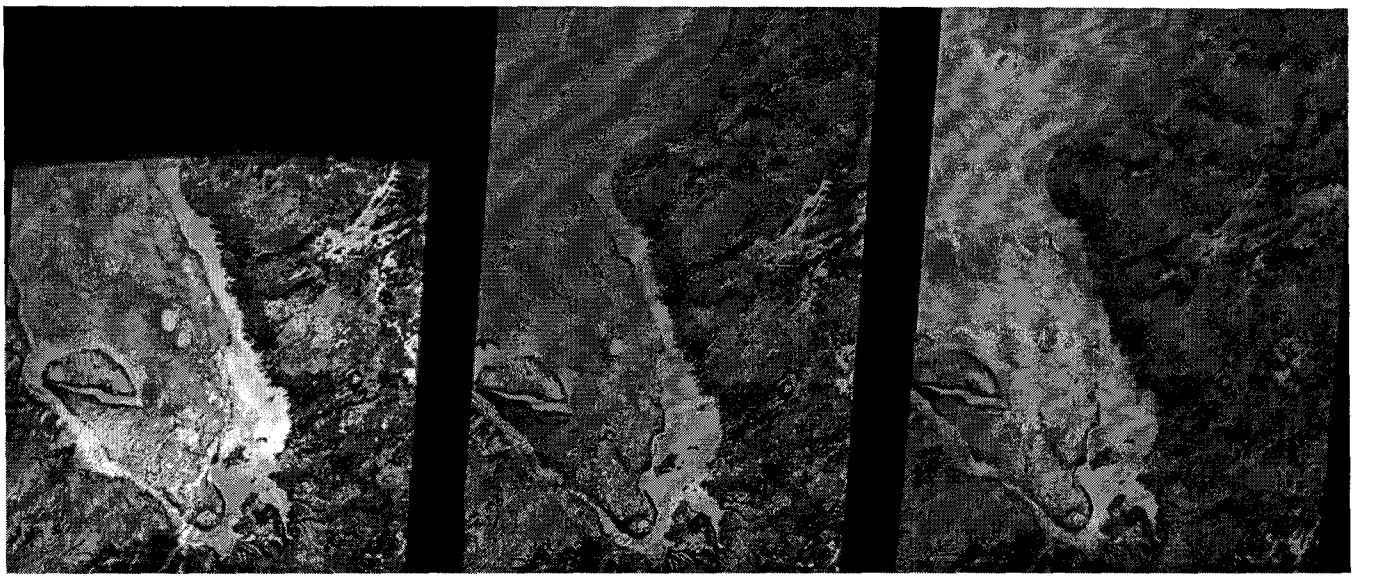

Figure 3. "First light" imagery obtained on February 24, 2000 over the ice-covered James Bay. The left image is from camera Df, the middle from An, and the right from Da. North is at the top.

Spatial co-registration of the 36 channels of data from the instrument is an essential requirement of all of the MISR geophysical retrievals. Since in-flight image collection began, calibration of the geometric model describing the pointing angles of the MISR cameras has been gradually improved through the use of ground control points. Using the camera model, image spatial co-registration is then accomplished during the routine ground data processing[2]. A common grid for the georectified radiances is established to provide the required co-registration. Space-Oblique Mercator (SOM) is used for this grid because its projection meridian nominally follows the spacecraft ground track and a constant distance scale is preserved along that track, thus minimizing distortion and resampling effects. The map resolution of the projection is matched to the horizontal sampling mode of each camera channel.

A separate projection is established for each of the paths of the 233 repeat orbits of the EOS 16-day cycle. The SOM-gridded images and geophysical data constitute an intermediate step to the Earth-based map projections to be used for global mapping at higher processing levels. Two types of SOM projection are used for MISR data: terrain projection, in which the images are mapped to a surface defined by a digital elevation model (DEM) in order to account for angle-dependent topographically induced misregistrations; and ellipsoid projection, in which the images are mapped to a surface defined by the WGS84 ellipsoid.

Figure 4 is a set of terrain-projected imagery acquired on August 25, 2000 and includes portions of Zambia and Botswana, Africa. The left image is a view from the vertical-viewing (nadir) camera. The distinctive fan-like feature on the left of each image is the highly vegetated Okavango Delta, a mosaicked network of grasslands and water channels, observed here during the dry season. The Zambezi River enters from the upper left and wends its way southeast, passing the Caprivi Strip, a narrow panhandle in northeast Namibia. The right image of Figure 4 is a composite of imagery from the nadir (An), 70.5° forward (Df), and 70.5° aftward (Da) cameras. An enlargement of a portion of this image, displayed in Figure 5, shows that using spacecraft-supplied attitude data and the calibrated camera geometric model enables imagery from different cameras, including the most oblique angles, to co-register with accuracies of a few hundred meters. This multi-angle compositing approach enables visualizing how different surface elements reflect light differently at different angles. The ability to construct such image composites at this spatial resolution is, to our knowledge, unique to MISR.

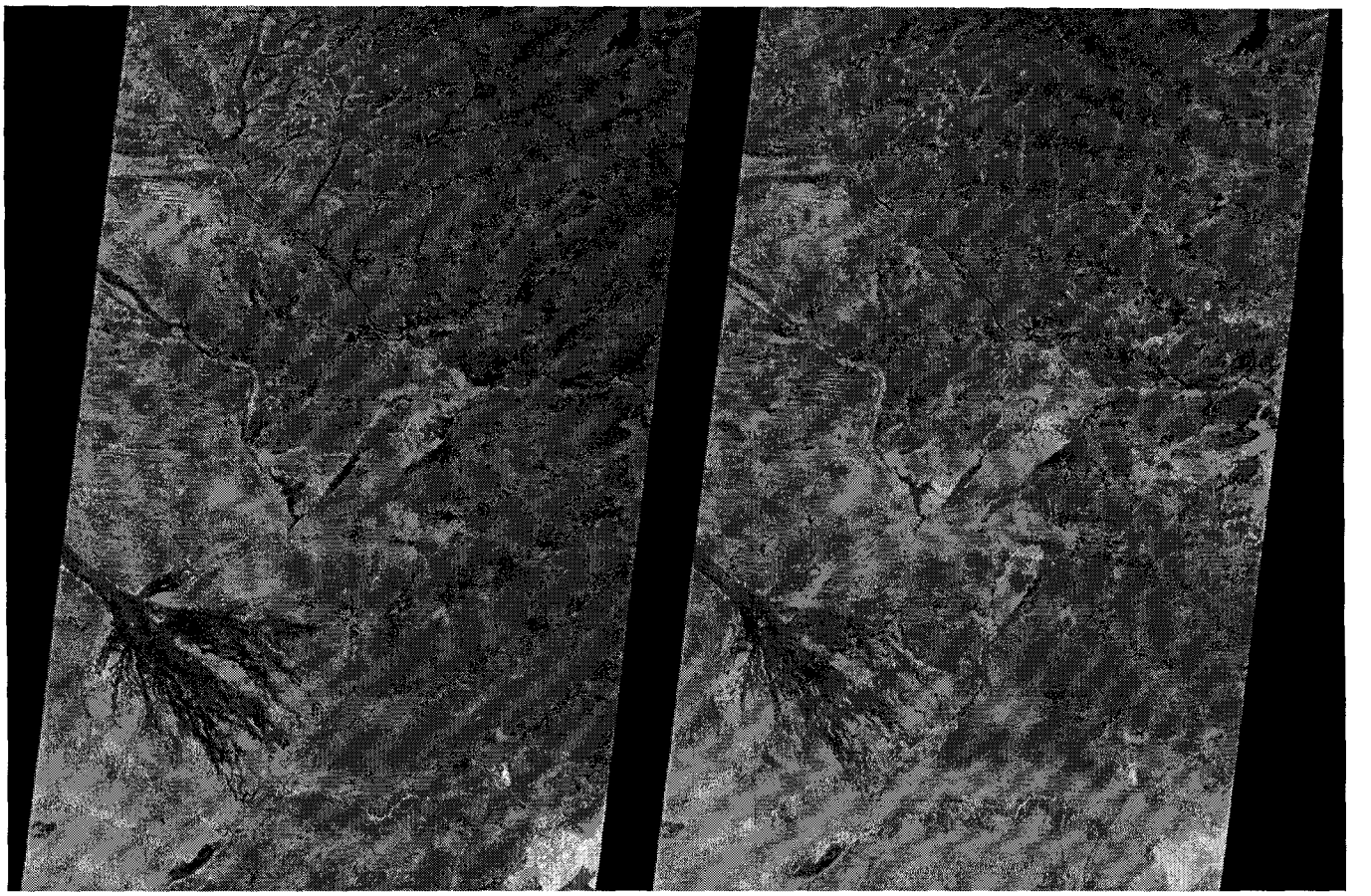

Figure 4. MISR imagery of Zambia and Botswana obtained on August 25, 2000. The left image is a superposition of three spectral bands from the An camera. The right image is a superposition of data from a single band (red), but from three different angles (An, Df, Da). North is at the top.

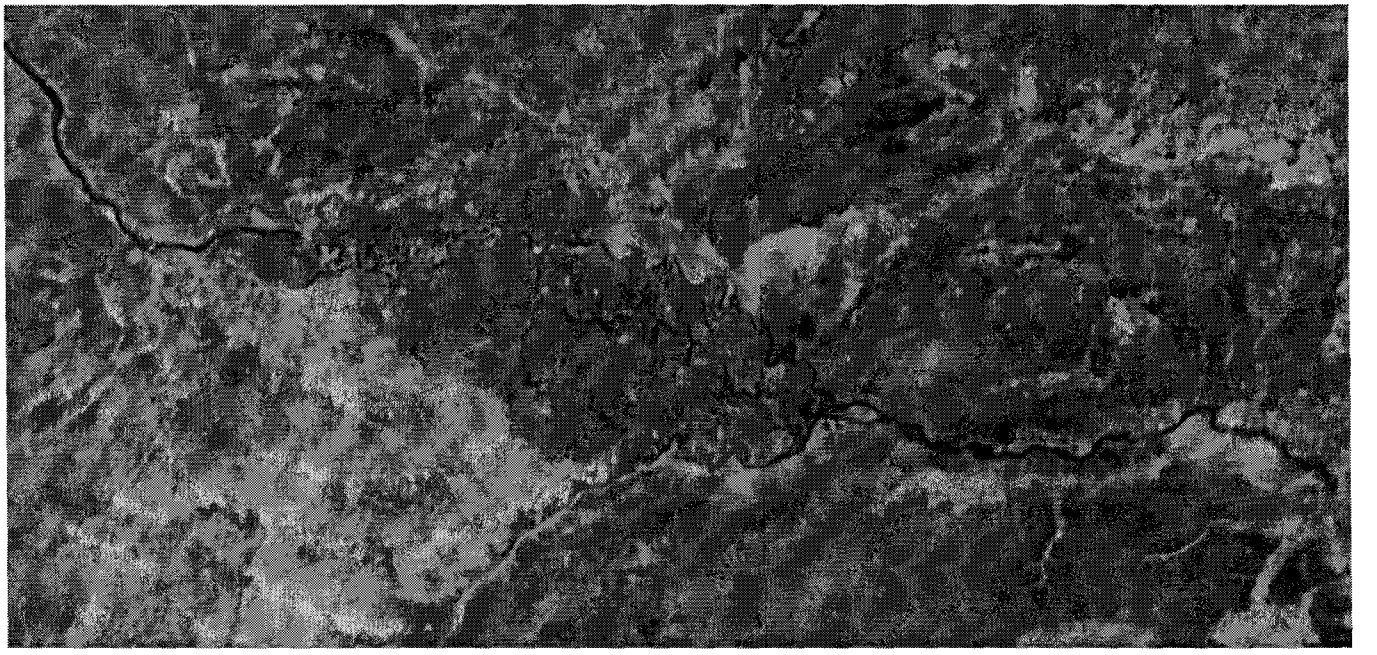

Figure 5. A 200-km-wide segment of the Zambezi Riverfrom the multi-angle composite image in Figure 4.

MISR operates continuously on the day side of every Terra orbit. This enables the instrument to capture a wide variety of terrestrial phenomena. For example, Figure 6, an image pair from a single orbit on August 14, 2000, shows two unrelated, large-scale natural events. The left image shows huge smoke plumes from devastating wildfires in the Bitterroot Mountain Range near the Montana-Idaho border. Flathead Lake is near the upper left, and the Great Salt Lake is at the bottom right. Smoke accumulating in the lower elevation canyons and plains is also visible. This image was generated from the Cf camera. The smoke is far more visible when seen at this highly oblique angle than it would be in a conventional, straight-downward (nadir) view. The wide extent of the smoke is evident from comparison with the image on the right, a view of Hurricane Hector acquired from the An camera. Both images are approximately 400 kilometers in width and about 850 kilometers in length. At the time the image of Hector was taken, this eastern Pacific tropical cyclone was located approximately 1100 kilometers west of the southern tip of Baja California, Mexico. The eye is faintly visible, and measures 25 kilometers in diameter. Convective activity was beginning to weaken at this time, and 24 hours later the National Weather Service downgraded Hector from a hurricane to a tropical storm.

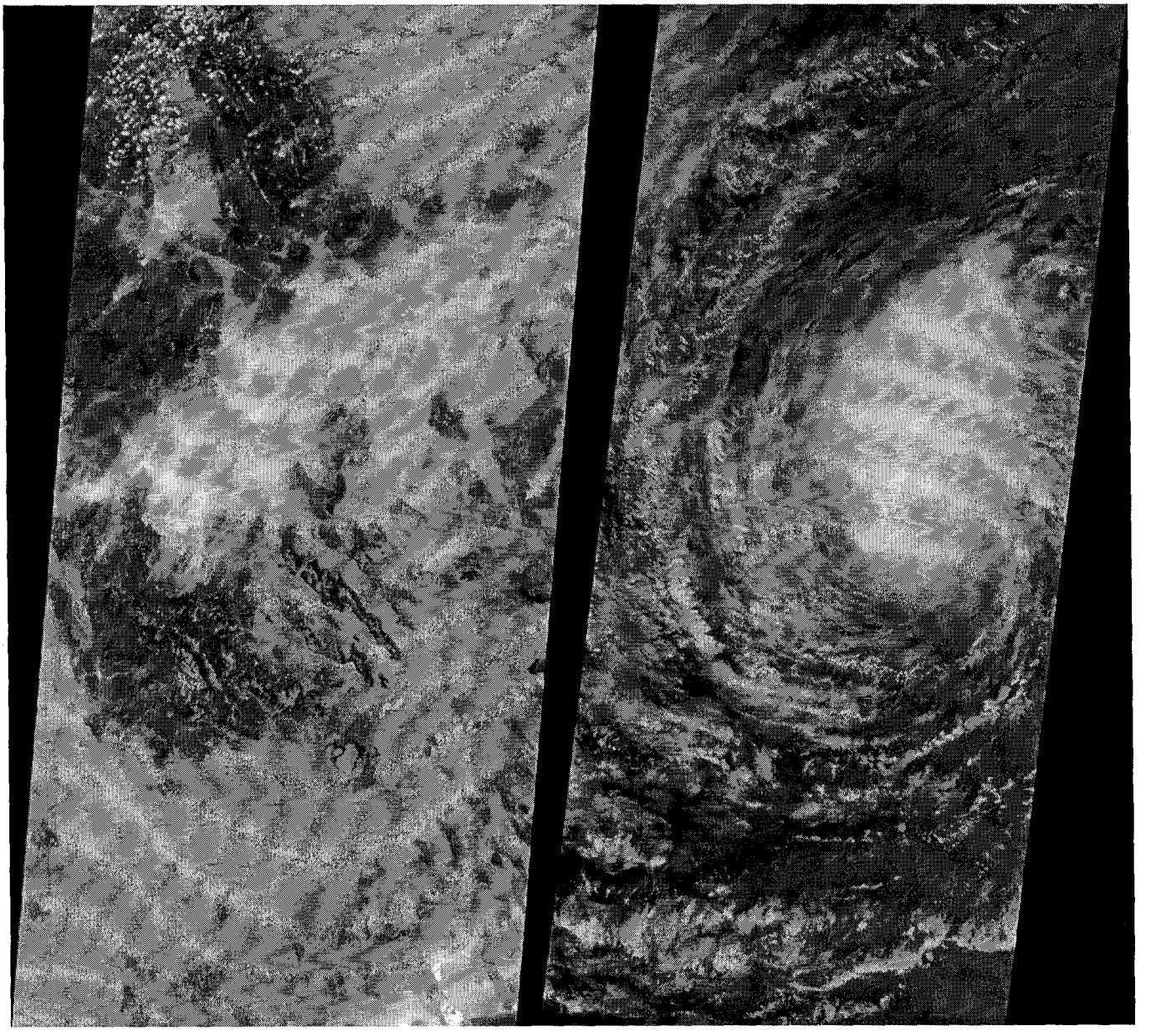

Figure 6. MISR imagery obtained on August 14, 2000. The left image is a Cf view of large smoke plumes from wildfires in Idaho and Montana. The image on the right is a nadir image of Hurricane Hector, acquired a short time later on the same orbit. North is at the top.

3. GEOPHYSICAL RETRIEVALS

3.1 Aerosol and Surface Retrieval Example

The retrieval of aerosol optical depth over land from space is a difficult challenge owing to the brightness and heterogeneity of the land surface. However, multi-angle imagery provides the opportunity to use the enhanced slant paths and variation in signal with angle to detect and characterize atmospheric hazes. One example of this capability is a set of images shown in Figure 7, obtained on March 6, 2000 over the eastern United States and encompassing Lake Ontario to Georgia. The left image is a nadir view, and the image immediately to the right is from camera Df. At the larger slant angle, the line-of-sight through the atmosphere is longer and a pall of haze over the Appalachian Mountains is significantly more apparent. The middle image is the result of an aerosol retrieval using a novel approach developed for MISR. This method requires the presence of spatial contrasts in the imagery and establishes a representation of the angular shape of the surface component of the reflectance using empirical orthogonal functions[3]. The aerosol optical depth is then derived from fitting the angular shape of the remaining signal to modeled atmospheric path radiances. Aerosol retrievals are performed on 17.6 x 17.6 km^2 regions, and thus at coarser resolution than the underlying imagery. In Figure 7, retrieved 558-nm optical depth in the hazier areas is ~0.2.

The results of the aerosol retrieval are used as input into a retrieval of surface parameters. Among these is the bihemispherical reflectance (BHR, one type of albedo). The next-to-the-last image in Figure 4 is a BHR retrieval performed by applying a correction only for ozone absorption and Rayleigh scattering. A residual due the aerosol is present. In the last (rightmost) image, the BHR retrieval has also included the retrieved aerosol. This process results in a "cleaner" surface retrieval.

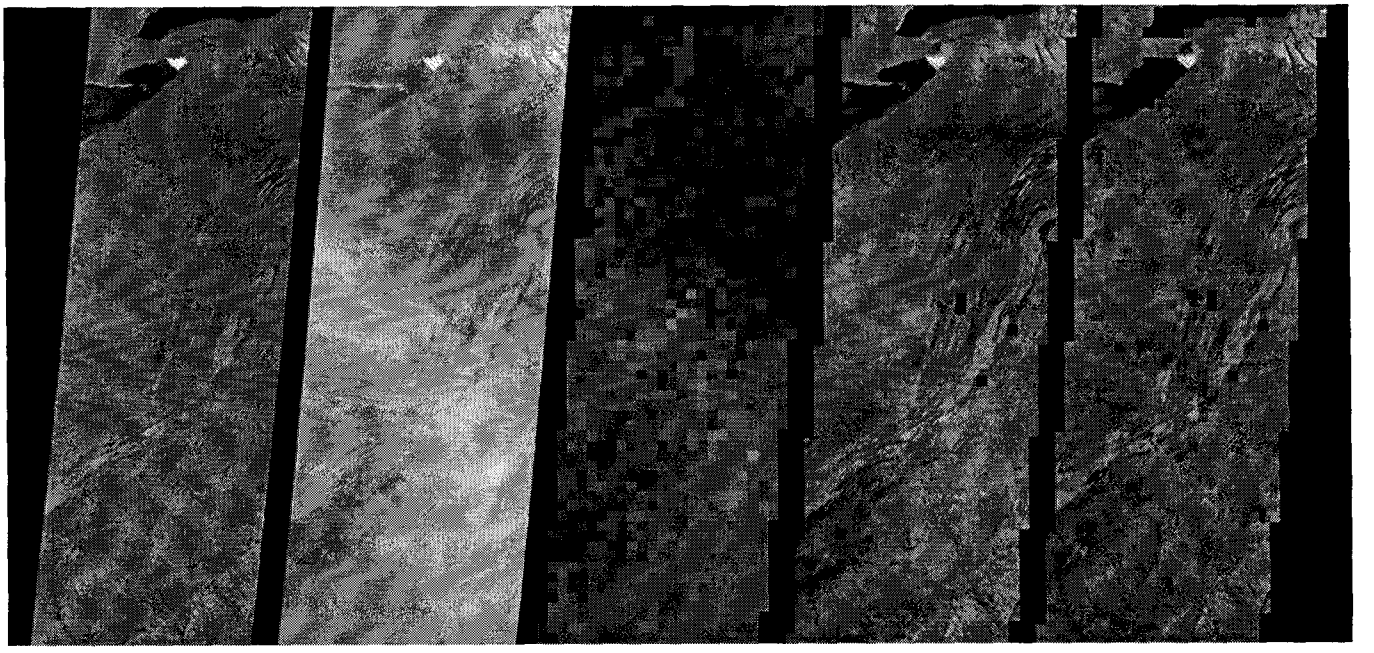

Figure 7. Data acquired over the eastern US, March 6, 2000. From left to right, An top-of-atmosphere (TOA) image, Df TOA image, retrieved 558-nm aerosol optical depth, retrieved surface BHR (ozone + Rayleigh correction only), retrieved surface BHR (ozone + Rayleigh + aerosol correction). North is at the top.

3.2 Cloud Retrieval Example

In studies of cloud-climate interactions, accurate cloud height is one of the principal characteristics required to model the three-dimensional field of radiative fluxes. In order to establish a classification scheme incorporating cloud altitudes, a reference level known as the Reflecting Level Reference Altitude is defined. The RLRA is the level found by matching features (or areas) with the greatest contrast in the near-nadir viewing directions. This corresponds to the main reflecting layer, which will typically be either the tops of clouds, or under clearer conditions, the surface. The RLRA is defined over areas measuring 2.2 km x 2.2 km^2.

The algorithm for retrieving RLRA is stereophotogrammetric, and uses a combination of area and feature matching algorithms to measure the displacement between clouds from one MISR view to another. This displacement results from geometric parallax due to the cloud's height above the surface ellipsoid, plus actual motion driven by wind. Multiple views obtained from satellite

altitude over a wide angular range provide the ability to separate the effects of wind displacement from height[4]. An example of RLRA retrieval is shown in Figure 8, derived from data acquired on March 6, 2000 (the simultaneous wind retrieval was not implemented in this processing run, so the quantitative values of the heights will change somewhat when this is done). The imagery has been rotated so that north is at the left. The top image is a nadir view, and includes portions of Florida, Cuba, Honduras, and Nicaragua. Below this image is the derived RLRA field. Brighter areas correspond to higher clouds.

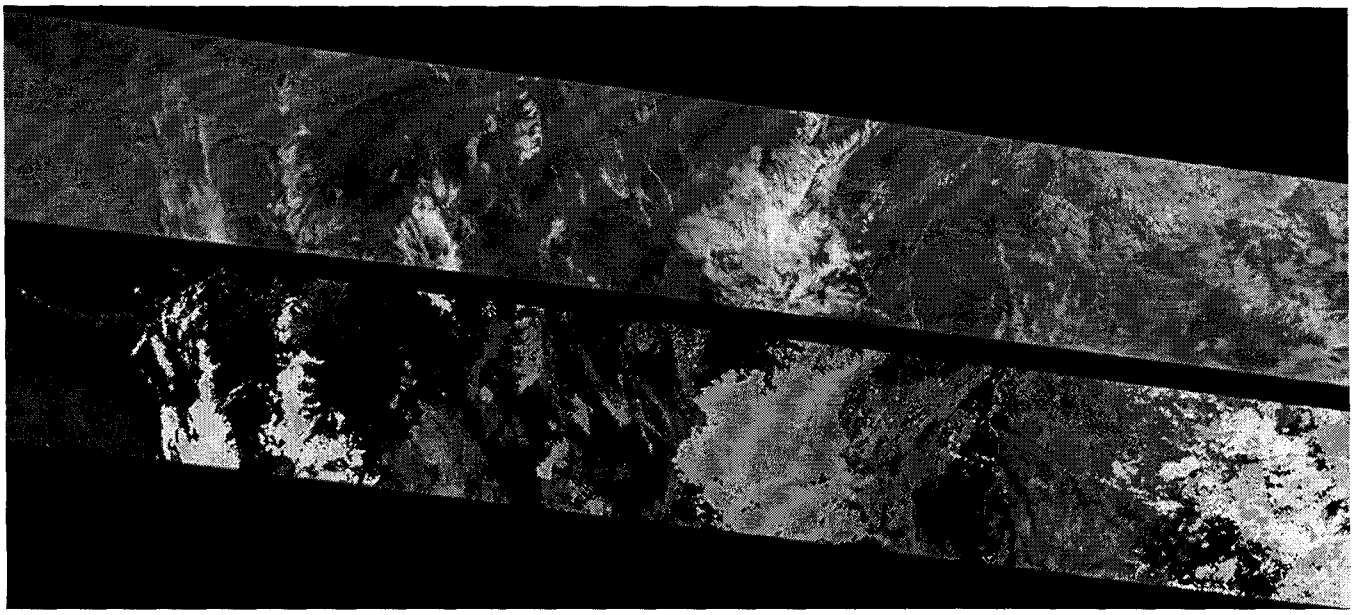

Figure 8. Top: Image acquired by the An camera on March 6, 2000, including parts of Florida, Cuba, Honduras, and Nicaragua. The data have been rotated such that north is at the left. Bottom: Retrieved RLRA. The brightest areas correspond to high cirrus near 10 km altitude, and darker shades of gray correspond to lower level clouds.

4. CONCLUSIONS

MISR is performing extremely well. Since June 2000, Level 1 data products, including calibrated, georectified, and co-registered MISR radiance imagery, as well as engineering data, have been publicly available at the LaRC DAAC (*http://eosweb.larc.nasa.gov*). Data access is through the EOS Data Gateway (EDG). Level 2 geophysical products are expected to be publicly available in Fall 2000. For further information, see *http://www-misr.jpl.nasa.gov*.

ACKNOWLEDGMENTS

We are grateful for the efforts of the entire MISR team. This work is being carried out at the Jet Propulsion Laboratory, California Institute of Technology, under contract with the National Aeronautics and Space Administration.

REFERENCES

1. D. Diner, J. Beckert, T. Reilly, C. Bruegge, J. Conel, R. Kahn, J. Martonchik, T. Ackerman, R. Davies, S. Gerstl, H. Gordon, J-P. Muller, R. Myneni, P. Sellers, B. Pinty, and M. Verstraete, "Multi-angle Imaging SpectroRadiometer (MISR) instrument description and experiment overview," IEEE Trans. Geosci. Rem. Sens. 36, pp. 1072-1087, 1998.

2. V.M. Jovanovic, M.M. Smyth, J. Zong, R. Ando, and G.W. Bothwell, "MISR photogrammetric data reduction for geophysical retrievals," IEEE Trans. Geosci. Rem. Sens. 36, pp. 1290-1301, 1998.

3. J.V. Martonchik, D.J. Diner, R.A. Kahn, T.P. Ackerman, M.M. Verstraete, B. Pinty, and H.R. Gordon, "Techniques for the retrieval of aerosol properties over land and ocean using multiangle imaging," IEEE Trans. Geosci. Rem. Sens. 36, pp. 1212-1227, 1998.

4. D.J. Diner, R. Davies, L. Di Girolamo, A. Horvath, C. Moroney, J-P. Muller, S.R. Paradise, D. Wenkert, and J. Zong, "MISR Level 2 Cloud Detection and Classification Algorithm Theoretical Basis," JPL Document D-11399, Rev. D, 1999. Available at *http://eospso.gsfc.nasa.gov/atbd/misrtables.html*.